NEUROSCIENCE

Dopamine neurons encode performance error in singing birds

Vikram Gadagkar, Pavel A. Puzerey, Ruidong Chen, Eliza Baird-Daniel,* Alexander R. Farhang,† Jesse H. Goldberg‡

Many behaviors are learned through trial and error by matching performance to internal goals. Yet neural mechanisms of performance evaluation remain poorly understood. We recorded basal ganglia–projecting dopamine neurons in singing zebra finches as we controlled perceived song quality with distorted auditory feedback. Dopamine activity was phasically suppressed after distorted syllables, consistent with a worse-than-predicted outcome, and was phasically activated at the precise moment of the song when a predicted distortion did not occur, consistent with a better-than-predicted outcome. Error response magnitude depended on distortion probability. Thus, dopaminergic error signals can evaluate behaviors that are not learned for reward and are instead learned by matching performance outcomes to internal goals.

When practicing piano, how do you know if you struck the right or wrong note? The problem is that there is nothing intrinsically "good" or "bad" about the sound of A-sharp. It entirely depends if that's the note you wanted to strike at that time step of the song. Performance evaluation requires sensory feedback to be compared with internal benchmarks that change from moment to moment in a sequence. Performance errors during musical performance (*1*, *2*) and speech production (*3*) are associated with a frontal error-related negativity in the electroencephalogram that may relate to activity in ventral tegmental area (VTA) dopamine neurons (*4*). Yet, although dopamine neurons are known to encode reward prediction error in tasks where animals seek primary rewards such as food or juice (*5*–*7*), it is not known if dopamine activity also encodes error in tasks that are not learned for primary reward and are instead learned by matching sensory feedback to internal performance benchmarks (*8*, *9*).

Songbirds use auditory feedback to learn to sing and have a dopaminergic projection from VTA to Area X, a nucleus required for song learning (*10*–*13*). It is hypothesized that a singing bird evaluates its own song to compute an auditory-error–based reinforcement signal that guides learning—i.e., a neural signal that "tells" vocal motor circuits if the recent vocalization was "good" and should be reinforced or "bad" and be eliminated (*14*, *15*) (Fig. 1A). The neural correlates of song evaluation remain unknown (*16*–*18*), leading to alternative models of learning that do not require online error signals (*19*).

To test if dopamine activity encodes performance error, we recorded songbird VTA neurons while controlling perceived song quality with distorted auditory feedback (DAF) (*18*, *20*–*24*) (Fig. 1, B to F). Beginning days before recordings, a specific song syllable was either distorted with DAF or, on randomly interleaved trials, left undistorted altogether (distortion rate 44 ± 8%, n = 26 birds; Fig. 1, E and F). DAF was a 50-ms snippet of sound with the same amplitude and spectral content as normal zebra finch song (see supplementary text). The snippet was either a segment of one of the bird's own syllables displaced in time (displaced-syllable DAF, n = 10 birds; Fig. 1E) or a synthesized sound designed to mimic broadband portions of the bird's own song (broadband DAF, n = 16 birds) (*20*, *24*). Operant broadband DAF drives dopamine and Area X–dependent reinforcement of undistorted syllable variants (*13*, *23*). Displaced-syllable DAF, when operantly delivered contingent on the pitch of a harmonic target syllable, resulted in similar learning (Fig. 1, G and H) (*20*).

To test for online error responses, we compared the activity between randomly interleaved renditions of distorted and undistorted songs. We computed the z-scored difference between target onset–aligned distorted and undistorted rate histograms (Fig. 2, A to D; target onset defined as the median DAF onset time relative to distorted syllable onset, n = 125 neurons in 26 birds) (*24*). We defined the error response as the average z-scored difference in firing in a 50- to 125-ms interval following target onset (*24*). We plotted the distribution of error responses across the 125 VTA neurons and observed two distinct groups: one that did not exhibit significant error responses (n = 108 neurons, error response 0.1 ± 0.9) and a group of error-responding neurons (n = 17 neurons, error response 3.3 ± 0.5; Fig. 2, E and F) that formed a distinct cluster ($P < 0.001$, bootstrap) (*24*). These two groups, defined as VTAerror (n = 17) and VTAother (n = 108), were spatially intermingled (fig. S1).

All VTAerror neurons were phasically suppressed by DAF during singing (Fig. 2, A to D, G; $P < 0.05$ in 17 out of 17 VTAerror neurons, bootstrap). Suppressions followed DAF onset with a latency of 58 ± 13 ms, lasted 86 ± 35 ms, and resulted on average in a 75% reduction in firing rate (range: 45 to 100%) (*24*, *25*). DAF-induced suppressions during singing were highly reliable, occurring on an average of 94% of distorted trials (range: 82 to 100%). VTAerror neurons also exhibited phasic activations following the precise time-step of undistorted songs where DAF would have occurred but did not occur (Fig. 2, A to D, G, and I; $P < 0.05$ in the same 17 neurons that exhibited suppressions on distorted trials, bootstrap). Phasic activations mirrored the phasic suppressions: They followed target onsets with a latency of 51 ± 20 ms, lasted 62 ± 27 ms, and resulted on average in a 77% (range: 42 to 214%) increase in firing rate (*24*) (Fig. 2H).

These precisely timed phasic activations suggest that undistorted target syllables are signaled as better than predicted, as if they are evaluated against an estimate of syllable quality that is diminished by a memory of errors (i.e., a flexible performance benchmark; see supplementary text). To test if error signals are scaled by error history, we trained 10 birds in a two-target paradigm in which one syllable was distorted with a high probability (target-1, 49 ± 4%) and a second syllable with low probability (target-2, 20 ± 4%) (Fig. 3, A to C) (*24*). The magnitude and reliability of phasic suppressions did not depend on error probability (percentage of suppression: target-1: 59%, range 45 to 77%; target-2: 63%, range 20 to 100%; reliability: target-1: 90%, range 82 to 100%; target-2: 86%, range 71 to 100%, $P > 0.4$, rank sum tests; Fig. 3D), consistent with weak scaling of dopaminergic negative reward prediction error responses (*6*, *7*). In contrast, phasic activations were significantly larger following (the more surprising) undistorted renditions of the high-probability target (increase in firing rate, target-1: 67%, range 42 to 159%; target-2: 22%, range −3 to 48%, $P < 0.001$, rank sum test; Fig. 3E). Error responses to target-2 did not depend on whether or not the preceding target-1 was distorted and vice versa, indicating that song time steps are independently evaluated against temporally aligned performance benchmarks ($P > 0.05$, rank sum tests and fig. S2).

More than 95% of Area X–projecting VTA neurons are dopaminergic (*11*). Fourteen of 125 VTA neurons were antidromically identified as projecting to Area X (Fig. 1, B to D), and 13 out of 14 VTAx neurons encoded performance error (Fig. 2, E and F). Firing patterns of VTAerror neurons were like those of mammalian dopamine neurons (see supplementary text and figs. S3 to S5).

Dopamine activity correlates with movement (*26*, *27*). We quantified movement with microdrive-mounted accelerometers (fig. S6 and movie S1). The activity of many VTA neurons was modulated by movement, which was in turn correlated with singing. But movement patterns during singing were not affected by DAF, and error responses were not affected by movement (n = 26 out of 26 birds, $P > 0.05$, bootstrapped d' analysis, see supplementary text, tables S1 and S2, and figs. S6 to S10).

Department of Neurobiology and Behavior, Cornell University, Ithaca, NY 14853, USA.
*Present address: Department of Neurological Surgery, Weill Cornell Medical College, New York, NY 10065, USA. †Present address: Department of Anatomy, University of California, San Francisco, CA 94143, USA. ‡Corresponding author. Email: jessehgoldberg@gmail.com

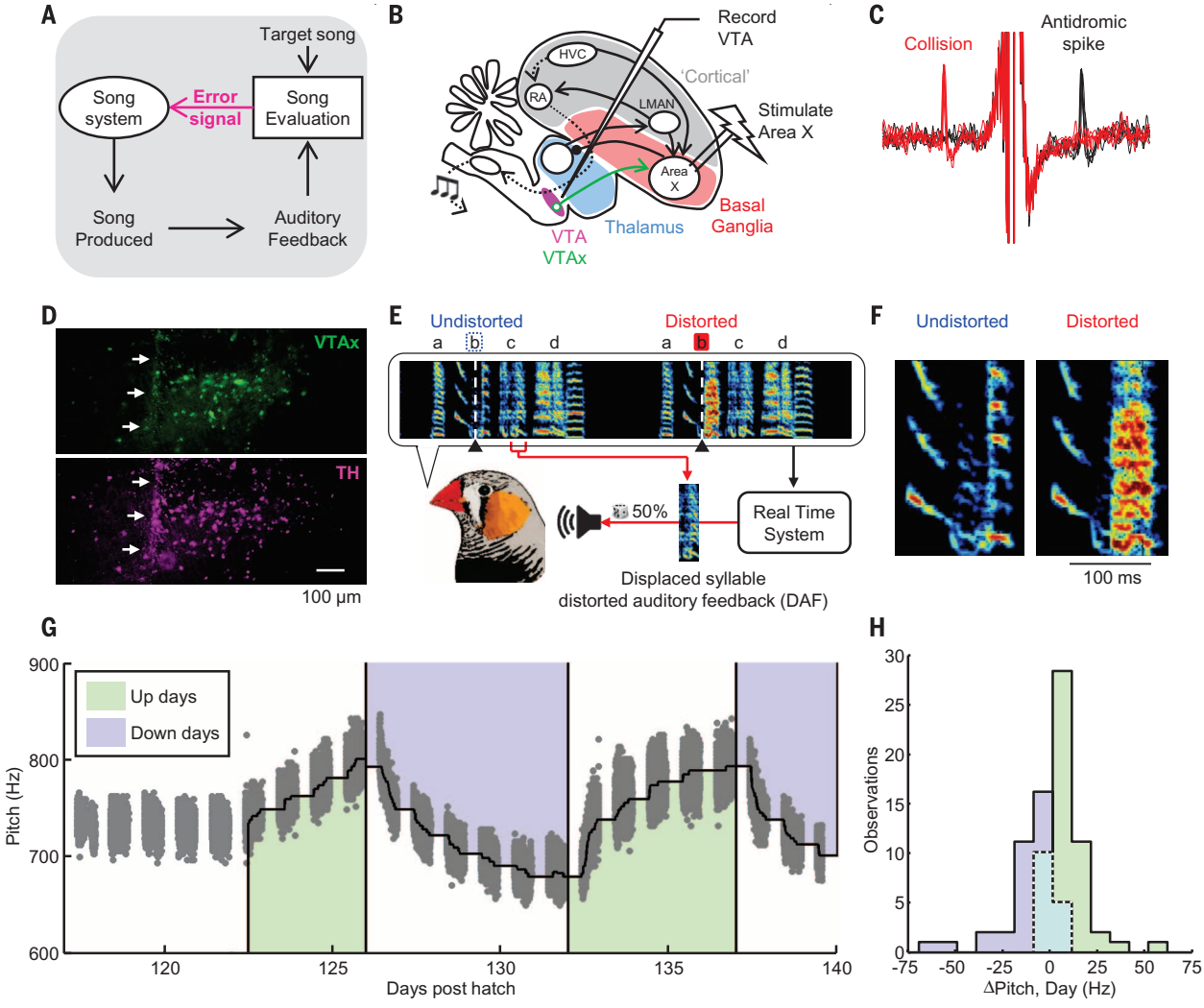

Fig. 1. Experimental test of performance error signals in birdsong. (**A**) Evaluation of auditory feedback during singing is hypothesized to result in "error" signals that reach the song system. (**B**) Strategy for antidromic identification of VTAx dopamine neurons. (**C**) Antidromic spikes (black) and spike collisions (red) of a VTAx neuron. (**D**) VTAx neurons labeled by injection of retrograde tracer into Area X (green, top) and colabeled dopamine neurons stained with antibody against tyrosine hydroxylase (TH) (purple, bottom). White arrows point to the visible path of the electrode that recorded the VTAx unit shown in Fig. 2A (scale bar, 100 µm; anterior-right, dorsal-top). (**E**) Example of displaced-syllable DAF. A snippet of syllable "c" was played back during production of the target syllable "b" (target time, black triangles and white dashed lines). Randomly interleaved target renditions were left undistorted (undistorted trials, blue dashed line). (**F**) Expanded view of the target syllable. (**G**) Pitch-contingent displaced-syllable DAF drives learning. Gray dots denote mean pitch of 49,716 target syllable renditions sung over 23 days for one bird. Shading demarcates distorted renditions; green, low-pitch variants distorted (up days); blue, high-pitch variants distorted (down days). (**H**) Histogram of pitch changes learned during each day (n = 4 birds).

VTAerror neurons might encode not performance error but simply the presence or absence of DAF as if it were an aversive stimulus (see supplementary text). An aversive response should persist in birds during nonsinging periods, whereas performance error should be restricted to singing. During nonsinging periods, VTAerror neurons did not differentially respond to playback of distorted and undistorted renditions of the bird's own song (normalized firing rate, distorted: 1.0 ± 0.2; undistorted: 1.1 ± 0.1; $P > 0.3$, unpaired t test) (Fig. 4) and did not exhibit pauses in response to DAF (fig. S11). Confinement of VTAerror responses to singing is consistent with performance error.

Performance error signals during singing are similar to prediction error signals during reward seeking (*5*). Suppression of VTAerror activity after distorted syllables resembles the dopamine response to worse-than-predicted reward outcomes. Activation of VTAerror neurons after undistorted syllables resembles the dopamine response to better-than-predicted reward outcomes. The scaling of positive VTAerror responses according to error history suggests that song is evaluated against flexible performance benchmarks. Positive reward prediction error signals are also scaled by reward prediction (*6*, *7*). Finally, performance and reward prediction error signals could underlie similar learning mechanisms. Dopamine-modulated corticostriatal plasticity links external stimuli to reward-maximizing responses (*14*). Dopamine-modulated corticostriatal plasticity also exists inside Area X (*28*) and could similarly link each time step in the song to the specific vocalization that produces a favorable outcome when produced at that time step (supplementary text and fig. S12). Such a mechanism would explain the reinforcement of undistorted syllable variants in operant DAF paradigms (Fig. 1, G and H) (*18*, *20*, *21*, *23*) and could contribute to natural song learning (*14*).

Yet, unlike reward prediction error, performance error during singing is not derived from sensory feedback of intrinsic reward or reward-predicting

value. The absence of error responses in birds passively hearing distorted or undistorted syllables suggests that there is nothing intrinsically "good" or "bad" about these sounds according to the performance-monitoring system. Performance error might instead derive from evaluation of auditory feedback against internal performance benchmarks that require, at each time step of the song sequence, information about the desired

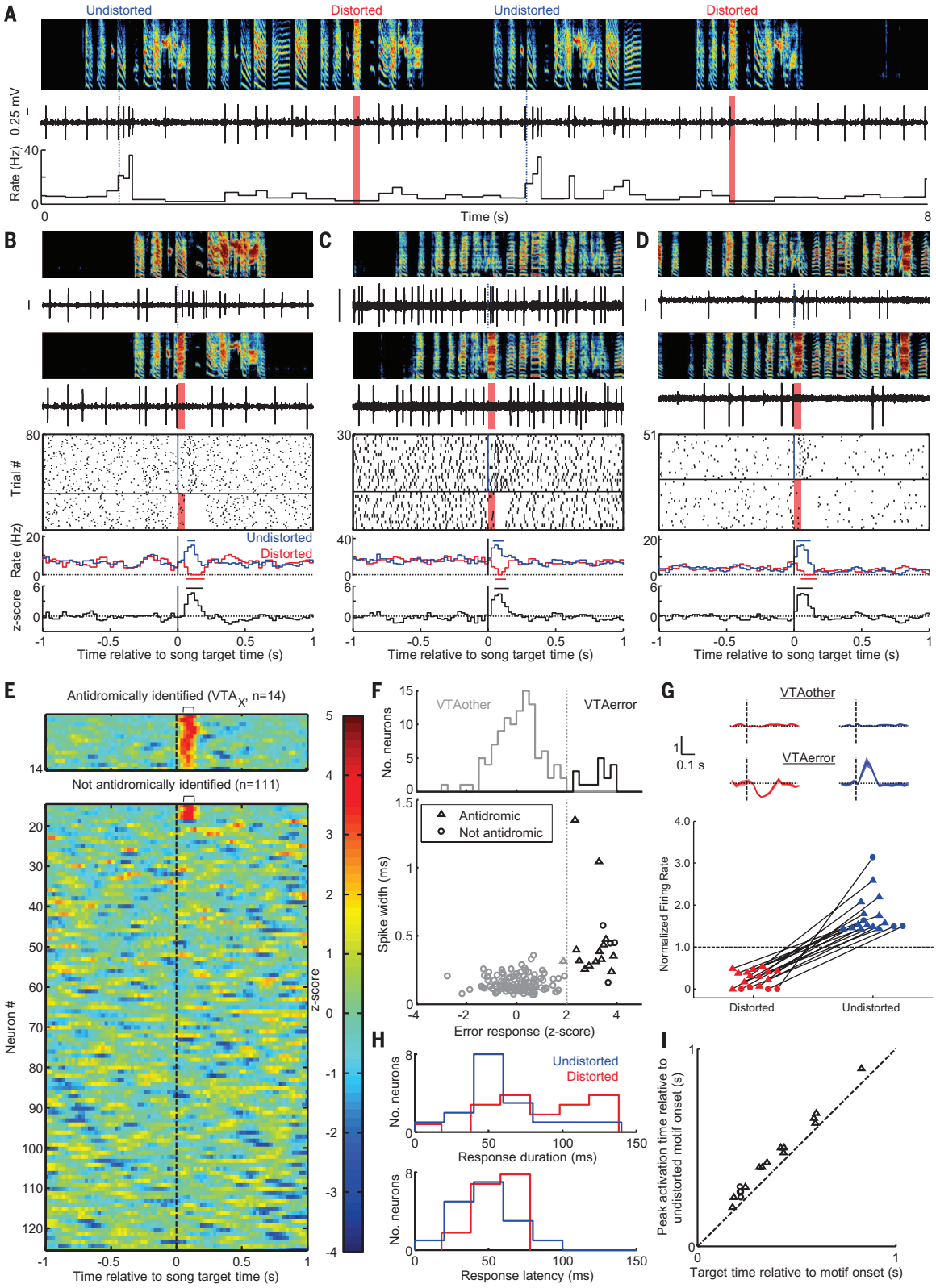

Fig. 2. VTA neurons encode performance error during singing. (**A**) Spectrogram, voltage trace, and the instantaneous firing rate of a VTAx neuron (DAF, red shading; undistorted targets, blue lines). (**B**) Top to bottom: spectrograms, spiking activity during undistorted and distorted trials, corresponding spike raster plots and rate histograms, and *z*-scored difference between undistorted and distorted rate histograms (plots aligned to target onset). Horizontal bars in histograms indicate significant deviations from baseline ($P < 0.05$, *z* test) (*24*). (**C** and **D**) Two additional VTAerror neurons as in (B). (**E**) Each row plots the *z*-scored difference between undistorted and distorted target-aligned rate histograms. VTAx neurons (top, $n = 14$) and non-antidromic neurons (bottom, $n = 111$) are independently sorted by maximal *z* score. (**F**) Top, distribution of error responses (*24*). Bottom, spike width versus error response (triangles: antidromic; circles: nonantidromic neurons). (**G**) Normalized response to distorted and undistorted targets (mean ± SEM) for VTAother (top) and VTAerror neurons (middle). Bottom, scatterplot of normalized rate in the 50 to 125 ms following distorted and undistorted trials (solid fills indicate $P < 0.05$, bootstrap). (**H**) Distributions of phasic response durations (top) and latencies (bottom). (**I**) For each VTAerror neuron, the time of maximal firing rate relative to motif onset is plotted against target time.

outcome, the actual outcome, and also the predicted probability of achieving the desired outcome. It remains unknown how upstream circuits construct the VTAerror signal. Multiple auditory cortical areas, including one that projects to VTA, respond to DAF specifically during singing (*22*, *25*), providing a candidate pathway for auditory mismatch signals to reach VTA. A newly identified Area X–basal forebrain–VTA pathway (*29*) might additionally provide a temporally precise and syllable-specific memory of errors required to compute a benchmark against which mismatch error signals are scaled.

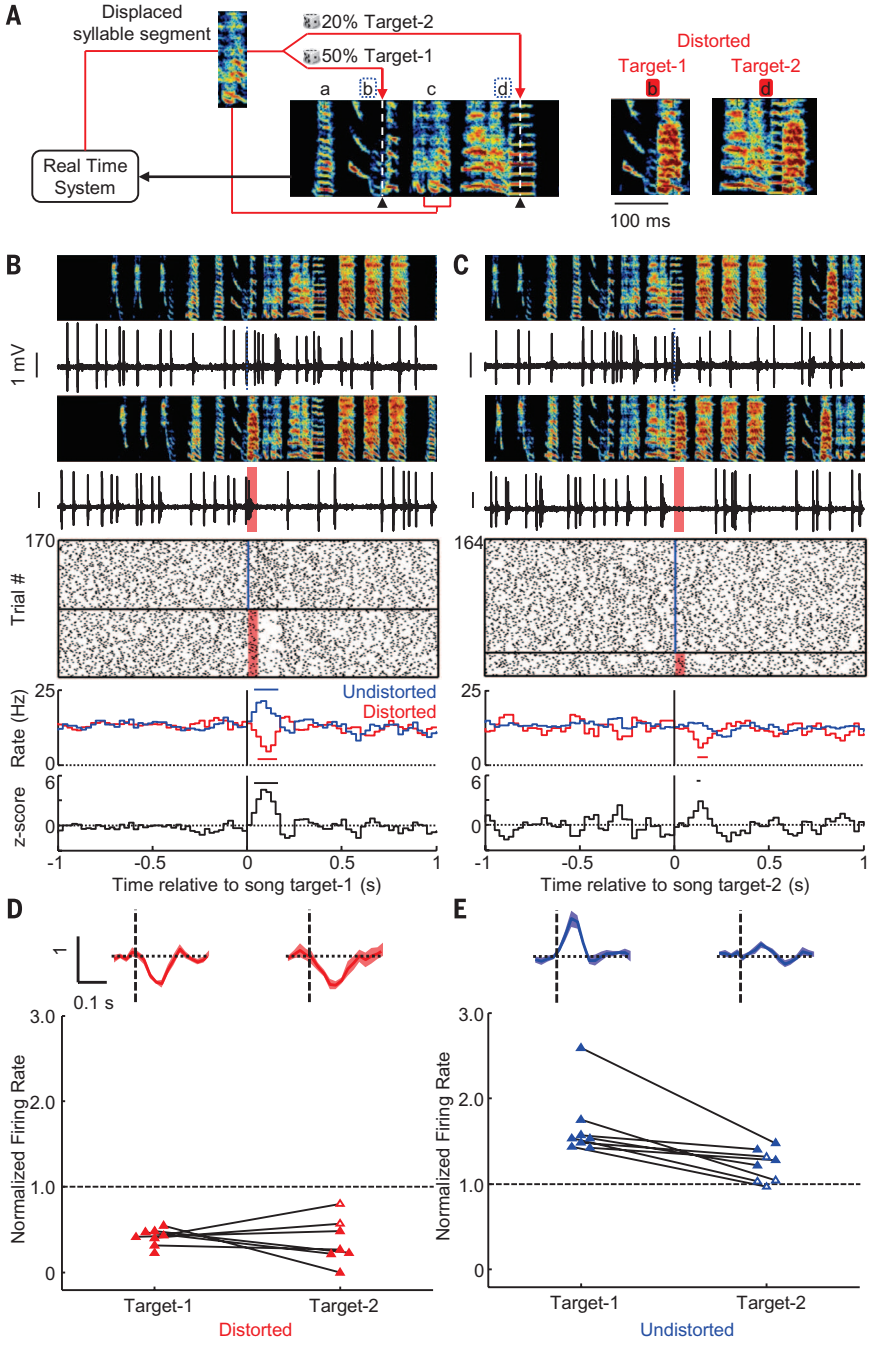

Fig. 3. VTAerror responses depend on error probability. (**A**) Displaced-syllable DAF scheme with two targets per motif (syllable b: target-1, distortion rate 50%; syllable d, target-2, distortion rate 20%; target times marked with dashed white line and black triangle). The distorted versions of the two target syllables are shown at right (color scheme as in Fig. 1E). (**B**) Target-1 and (**C**) target-2 error responses for the same neuron. Top to bottom: spectrograms, spiking activity during undistorted and distorted trials, corresponding spike raster plots and rate histograms, and *z*-scored difference between undistorted and distorted rate histograms (all plots aligned to target onset). Horizontal bars in histograms indicate significant deviations from baseline ($P < 0.05$, *z* test) (*24*). (**D**) Top, normalized responses to distorted targets (mean ± SEM) for VTAerror neurons. Bottom, scatterplot of normalized rate in the 50 to 125 ms following target time (solid fills indicate $P < 0.05$, bootstrap). (**E**) Same as (D) but for undistorted targets.

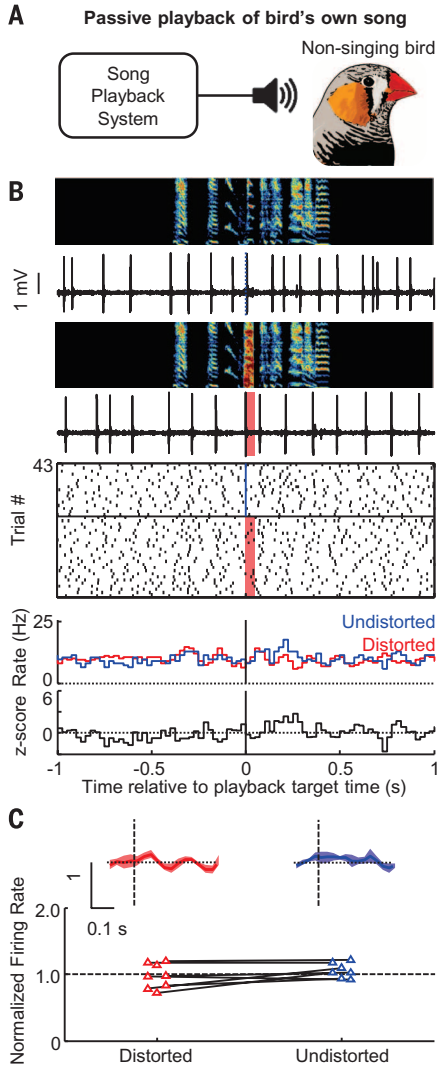

Fig. 4. Response of VTAerror neurons to birdsong during nonsinging. (**A**) Distorted and undistorted renditions of the bird's own song was played back during nonsinging periods. (**B**) Top to bottom: spectrograms, spiking activity of the VTAx neuron shown in Fig. 3 during playback of undistorted and distorted songs, corresponding spike raster plots and rate histograms, and *z*-scored difference between undistorted and distorted rate histograms (all plots aligned to target onset). (**C**) Normalized responses to distorted and undistorted targets (mean ± SEM) for VTAerror neurons during passive playback (top). Bottom, scatterplot of normalized rate in the 50 to 125 ms following target time (empty fills indicate no significant response, $P > 0.05$, bootstrap) (*24*).

REFERENCES AND NOTES

1. C. Maidhof, N. Vavatzanidis, W. Prinz, M. Rieger, S. Koelsch, *J. Cogn. Neurosci.* **22**, 2401–2413 (2010).
2. K. Katahira, D. Abla, S. Masuda, K. Okanoya, *Neurosci. Res.* **61**, 120–128 (2008).
3. K. M. Trewartha, N. A. Phillips, *Front. Hum. Neurosci.* **7**, 763 (2013).
4. C. B. Holroyd, M. G. Coles, *Psychol. Rev.* **109**, 679–709 (2002).
5. W. Schultz, P. Dayan, P. R. Montague, *Science* **275**, 1593–1599 (1997).
6. C. D. Fiorillo, P. N. Tobler, W. Schultz, *Science* **299**, 1898–1902 (2003).
7. H. M. Bayer, P. W. Glimcher, *Neuron* **47**, 129–141 (2005).
8. D. M. Wolpert, J. Diedrichsen, J. R. Flanagan, *Nat. Rev. Neurosci.* **12**, 739–751 (2011).
9. S. Singh, R. Lewis, A. Barto, J. Sorg, *IEEE Trans. Auton. Ment. Dev.* **2**, 70–82 (2010).
10. M. Konishi, *Z. Tierpsychol.* **22**, 770–783 (1965).
11. A. L. Person, S. D. Gale, M. A. Farries, D. J. Perkel, *J. Comp. Neurol.* **508**, 840–866 (2008).
12. C. Scharff, F. Nottebohm, *J. Neurosci.* **11**, 2896–2913 (1991).
13. L. A. Hoffmann, V. Saravanan, A. N. Wood, L. He, S. J. Sober, *J. Neurosci.* **36**, 2176–2189 (2016).
14. M. S. Fee, J. H. Goldberg, *Neuroscience* **198**, 152–170 (2011).
15. K. Doya, T. Sejnowski, *Adv. Neural Inf. Process. Syst.* **7**, 101–108 (1995).
16. A. Leonardo, *Proc. Natl. Acad. Sci. U.S.A.* **101**, 16935–16940 (2004).
17. A. A. Kozhevnikov, M. S. Fee, *J. Neurophysiol.* **97**, 4271–4283 (2007).
18. K. Hamaguchi, K. A. Tschida, I. Yoon, B. R. Donald, R. Mooney, *eLife* **3**, e01833 (2014).
19. R. Hahnloser, S. Ganguli, in *Principles of Neural Coding*, S. Panzeri, P. Quiroga, Eds. (CRC Taylor and Francis, Boca Raton, FL, 2013), pp. 547–564.
20. A. S. Andalman, M. S. Fee, *Proc. Natl. Acad. Sci. U.S.A.* **106**, 12518–12523 (2009).
21. E. C. Tumer, M. S. Brainard, *Nature* **450**, 1240–1244 (2007).
22. G. B. Keller, R. H. Hahnloser, *Nature* **457**, 187–190 (2009).
23. F. Ali *et al*., *Neuron* **80**, 494–506 (2013).
24. Materials and methods are available as supplementary materials on *Science* Online.
25. Y. Mandelblat-Cerf, L. Las, N. Denisenko, M. S. Fee, *eLife* **3**, e02152 (2014).
26. X. Jin, R. M. Costa, *Nature* **466**, 457–462 (2010).
27. M. W. Howe, D. A. Dombeck, *Nature* **535**, 505–510 (2016).
28. L. Ding, D. J. Perkel, *J. Neurosci.* **24**, 488–494 (2004).
29. S. D. Gale, D. J. Perkel, *J. Neurosci.* **30**, 1027–1037 (2010).

ACKNOWLEDGMENTS

We thank J. Fetcho, M. Warden, M. Long, A. Andalman, and D. Aronov for comments on the manuscript; J. Cohen for mouse VTA recording data; T. Bollu and D. Murdoch for technical support; J. Wu and K. Maher for histology; and A. Treska for art. Funding support was provided to J.H.G. by NIH (grant R01NS094667), Pew Charitable Trusts, and Klingenstein Neuroscience Foundation and to V.G. by Simons Foundation. V.G. and J.H.G. designed the research, analyzed the data, and wrote the paper. V.G., P.A.P., R.C., A.R.F., E.B.-D., and J.H.G. performed experiments. The authors declare no competing financial interests. Data can be accessed at www.nbb.cornell.edu/goldberg/.

SUPPLEMENTARY MATERIALS

www.sciencemag.org/content/354/6317/1278/suppl/DC1
Materials and Methods
Supplementary Text
Figs. S1 to S12
Tables S1 to S2
Movie S1
References (*30*–*68*)

1 August 2016; accepted 24 October 2016
10.1126/science.aah6837

NEUROSCIENCE

Mind the gap: Neural coding of species identity in birdsong prosody

Makoto Araki,[1] M. M. Bandi,[2] Yoko Yazaki-Sugiyama[1]*

Juvenile songbirds learn vocal communication from adult tutors of the same species but not from adults of other species. How species-specific learning emerges from the basic features of song prosody remains unknown. In the zebra finch auditory cortex, we discovered a class of neurons that register the silent temporal gaps between song syllables and are distinct from neurons encoding syllable morphology. Behavioral learning and neuronal coding of temporal gap structure resisted song tutoring from other species: Zebra finches fostered by Bengalese finch parents learned Bengalese finch song morphology transposed onto zebra finch temporal gaps. During the vocal learning period, temporal gap neurons fired selectively to zebra finch song. The innate temporal coding of intersyllable silent gaps suggests a neuronal barcode for conspecific vocal learning and social communication in acoustically diverse environments.

There are more than 5000 species of songbirds, each with unique species-selective acoustic features in their songs (*1*–*3*) after accounting for individual variance. The vocal characteristics of birdsongs are learned from early auditory experience with adult tutors within species-specific constraints (*4*). Juvenile birds learning to sing must simultaneously balance competing criteria: keeping their individual song distinct from conspecifics (*5*) while avoiding divergence beyond their own species' song identity (*6*, *7*). Both experience-dependent and innate mechanisms contribute to species-selective song learning (*8*). The observed behavioral discrimination of conspecific and heterospecific vocalizations suggests innate contributions to song learning (*9*–*12*). In the zebra finch, one song unique to each individual is learned during development. The songs comprise stereotyped repeats of a few syllables, called "song motifs," in which syllables are separated by silent gaps. The brain circuits that are necessary for song learning and production are well identified (*13*). However, the brain mechanisms for the detection of conspecific vocalization, while also accommodating individual differences in song learning, remain unknown.

We performed a cross-fostering experiment in which zebra finches were raised by Bengalese finch foster parents (X-fostered zebra finches) (*14*). Zebra finch song syllables, excluding introductory notes, showed bimodal distributions in length and were separated by silent gaps with durations of 20 to 100 ms (Fig. 1B and fig. S1A). Gaps longer than 200 ms are recognized as gaps between song bouts (*15*). In contrast, Bengalese finch songs included a larger number of syllables sung in variable sequence, and the distribution of syllable durations was shorter than in zebra finch songs (Fig. 1, A and B, and fig. S1, B and C). The probability distributions of the silent gap durations in Bengalese and zebra finch songs overlapped; however, Bengalese finch songs included a larger number of longer gaps (Fig. 1B and fig. S1C). X-fostered zebra finch juveniles learned Bengalese finch syllable morphologies (Fig. 1C; rate of copied syllables from tutor song was greater than rate of random matching with unrelated Bengalese finch songs; $P < 0.029$, paired t test) as well as syllable durations (Fig. 1D). The durations of tutor and copied juvenile syllables showed a linear correlation (slope = 0.94, r^2 = 0.907) and no significant difference ($P > 0.5$, paired t test, 44 ± 6 ms versus 43 ± 6 ms, mean ± SD). Even the difference in syllable duration histograms (Fig. 1B, bottom), measured by Kullback-Leibler distance, between X-fostered and normal zebra finch songs was similar to that between Bengalese finch and zebra finch songs, whereas the difference between X-fostered zebra finch and Bengalese finch songs was much smaller than that between zebra finch and Bengalese finch songs (fig. S1C; note that the Kullback-Leibler distance is order-sensitive). Furthermore, X-fostered zebra finch songs included more syllables than normal zebra finch songs (fig. S1B) but consisted of a clear motif, not a variable sequence.

Despite learning the syllable morphology of Bengalese finches, X-fostered zebra finches did not learn their temporal silent gaps. When they copied syllable chunks from Bengalese finch tutors, they truncated gaps that were longer than normal zebra finch gaps (>50 ms) but copied gaps that were similar to those of normal zebra finches (<50 ms) (Fig. 1E). Tutor gaps were significantly longer than copied juvenile gaps (P = 0.002, paired t test, 51 ± 6 ms versus 38 ± 3 ms, mean ± SD). The slope of the correlation between tutor and copied juvenile gap duration was shallower than for syllable duration (Fig. 1E; slope = 0.42, r^2 = 0.640). The distribution of gap duration in X-fostered zebra finch songs also remained closer to that of zebra finch songs, which typically do not involve gaps greater than 80 ms (Fig. 1B and fig. S1C). The difference in the histograms of gap duration probability between X-fostered and normal zebra finch songs was much

[1]Neuronal Mechanism of Critical Period Unit, Okinawa Institute of Science and Technology (OIST) Graduate University, Okinawa, Japan. [2]Collective Interactions Unit, OIST Graduate University, Okinawa, Japan.
*Corresponding author. Email: yazaki-sugiyama@oist.jp

Science

Dopamine neurons encode performance error in singing birds

Vikram GadagkarPavel A. PuzereyRuidong ChenEliza Baird-DanielAlexander R. FarhangJesse H. Goldberg

Science, 354 (6317), • DOI: 10.1126/science.aah6837

Birds of a feather sing together

How do birds know that a song that they hear is from a member of their own species, and how do they learn their songs in the first place? Araki *et al.* identified two types of brain cells involved in how finches learn their songs (see the Perspective by Tchernichovski and Lipkind). When zebra finches were raised by Bengalese finch foster parents, they learned a song whose morphology resembled that of their foster father. However, the temporal structure remained zebra finch–specific, suggesting that it is innate. Gadagkar *et al.* recorded activity in specific dopamine neurons in singing zebra finches while controlling perceived song quality with distorted auditory feedback. This distorted feedback represented worse performance than predicted and resulted in negative prediction errors. These findings suggest again that finches have an innate internal goal for their learned songs.

Science, this issue p. 1282, p. 1234; see also p. 1278

Science (ISSN 1095-9203) is published by the American Association for the Advancement of Science. 1200 New York Avenue NW, Washington, DC 20005. The title *Science* is a registered trademark of AAAS.